Journal of Theoretical Biology 404 (2016) 1–9

Contents lists available at ScienceDirect

Journal of Theoretical Biology

journal homepage: www.elsevier.com/locate/yjtbi

Improving dynamic phytoplankton reserve-utilization models with an indirect proxy for internal nitrogen

Martino E. Malerba [a,b,c,*], Kirsten Heimann [c,d], Sean R. Connolly [c,e]

[a] AIMS@JCU, James Cook University, Townsville, Queensland 4811, Australia
[b] Australian Institute of Marine Science, Townsville, Queensland 4811, Australia
[c] College of Marine and Environmental Sciences, James Cook University, Townsville, Queensland 4811, Australia
[d] Centre for Sustainable Tropical Fisheries and Aquaculture, Townsville, Queensland 4811, Australia
[e] Australian Research Council Centre of Excellence for Coral Reef Studies, James Cook University, Townsville, Queensland 4811, Australia

HIGHLIGHTS

- Per-cell red fluorescence is a proxy for internal nitrogen in phytoplankton cells.
- We propose to use red fluorescence to improve models on cell nutrient utilization.
- Red fluorescence was tested to substantially improve the performance of Quota models.
- This is a new way to model cell growth while accounting for storage mechanisms.

ARTICLE INFO

Article history:
Received 3 January 2016
Received in revised form
10 May 2016
Accepted 16 May 2016
Available online 20 May 2016

Keywords:
Quota
Nitrogen limitation
Phytoplankton
Cell nutrient status
Ecological modelling
Allometric scaling
State-space models
Dynamic models
Markov Chain Monte Carlo (MCMC)
Stochastic simulations

ABSTRACT

Ecologists have often used indirect proxies to represent variables that are difficult or impossible to measure directly. In phytoplankton, the internal concentration of the most limiting nutrient in a cell determines its growth rate. However, directly measuring the concentration of nutrients within cells is inaccurate, expensive, destructive, and time-consuming, substantially impairing our ability to model growth rates in nutrient-limited phytoplankton populations. The red chlorophyll autofluorescence (hereafter "red fluorescence") signal emitted by a cell is highly correlated with nitrogen quota in nitrogen-limited phytoplankton species. The aim of this study was to evaluate the reliability of including flow cytometric red fluorescence as a proxy for internal nitrogen status to model phytoplankton growth rates. To this end, we used the classic Quota model and designed three approaches to calibrate its model parameters to data: where empirical observations on cell internal nitrogen quota were used to fit the model ("Nitrogen-Quota approach"), where quota dynamics were inferred only from changes in medium nutrient depletion and population density ("Virtual-Quota approach"), or where red fluorescence emission of a cell was used as an indirect proxy for its internal nitrogen quota ("Fluorescence-Quota approach"). Two separate analyses were carried out. In the first analysis, stochastic model simulations were parameterized from published empirical relationships and used to generate dynamics of phytoplankton communities reared under nitrogen-limited conditions. Quota models were fitted to the dynamics of each simulated species with the three different approaches and the performance of each model was compared. In the second analysis, we fit Quota models to laboratory time-series and we calculate the ability of each calibration approach to describe the observed trajectories of internal nitrogen quota in the culture. Results from both analyses concluded that the Fluorescence-Quota approach including per-cell red fluorescence as a proxy of internal nitrogen substantially improved the ability of Quota models to describe phytoplankton dynamics, while still accounting for the biologically important process of cell nitrogen storage. More broadly, many population models in ecology implicitly recognize the importance of accounting for storage mechanisms to describe the dynamics of individual organisms. Hence, the approach documented here with phytoplankton dynamics may also be useful for evaluating the potential of indirect proxies in other ecological systems.

* Corresponding author at: College of Marine and Environmental Sciences, James Cook University, Townsville, Queensland 4811, Australia.
E-mail address: Martino.Malerba@gmail.com (M.E. Malerba).

http://dx.doi.org/10.1016/j.jtbi.2016.05.023
0022-5193/

1. Introduction

Proxy variables are commonly used in ecology as a way to quantify processes that would otherwise be difficult or impossible to monitor directly (Caro, 2010; Lindenmayer et al., 2015). For instance, indirect proxies can facilitate recording abundance data (Eigenbrod et al., 2010; Stephens et al., 2015). This is especially true for vegetation models, where indirect optical proxies for different canopy attributes (e.g. net primary production, plant biomass, photosynthetically active radiations) have played a crucial role overcoming many long-standing monitoring challenges, for example evaluation of impervious regions, such as the Arctic and Antarctic (Santin-Janin et al., 2009; Epstein et al., 2012), or fragmented and isolated areas (Pereira Coltri et al., 2013; Li et al., 2014), or very extended territories (Son et al., 2014; Stephens et al., 2015). Another use of indirect proxies in ecology is to quantify the overall performance of a species. For instance, trait-based approaches use different types of measurable eco-physiological and life-history traits (e.g. growth, body mass, fecundity) to make inferences about the ecological capabilities of a species (e.g. competitive ability) and about complex processes at higher organizational levels (e.g. community structure, ecosystem functioning, energy flow: McGill et al., 2006; Violle et al., 2007). For example, the colony shape of a coral species is a proxy for its susceptibility to mortality from physical dislodgment (Madin et al., 2014). Proxies can also be used to quantify the condition of an individual organism. For instance, the size of the liver and its lipid concentration is a good proxy for the health of a fish (Dempster et al., 2011). Also, whole-organism oxygen consumption rate is a traditional proxy for metabolic activity or energy consumption (Brown et al., 2004; Salin et al., 2015) and various biochemical indices have been used as proxies for specific growth rate and overall activity of an organism (Runge and Roff, 2000; Holmborn et al., 2009). Hence, indirect proxies serve different purposes in ecology across different scales, ranging from biomes, to species, and to individuals.

The use of indirect proxies is particularly important when studying organisms that are difficult to measure directly, such as phytoplankton. The productivity of phytoplankton populations is critical to sustain life on the planet, and their rate of cell division is often regulated by the availability of inorganic nutrients to a cell. However, phytoplankton cells are also adapted to store nutrients to support growth in periods of low nutrient availability (Caperon and Meyer, 1972; Droop, 1973, 1983), which complicates the analysis of nutrient utilization and population dynamics. Quota models are the most successful representation of phytoplankton nutrient utilization to date, because of their ability to incorporate internal nutrient storage within single cells that can temporarily support cell division even in the absence of sufficient external nutrients (Droop, 1973; Leadbeater, 2006; Pahlow and Oschlies, 2013). The key assumption of Quota models is largely biologically justified: phytoplankton cells are adapted to respond to nutrient-limited conditions by relocating resources from storage molecules (e.g. lipids, carbohydrates, pigments, RNA) to vital metabolic functions (e.g. cell division; Dortch et al., 1984). However, analysing phytoplankton nutrient utilization by fitting Quota models to data also requires monitoring the internal nutrient status of a cell, which is the most stringent limitation to this modelling technique. Estimating nutrient concentrations within phytoplankton cells is technically complicated, costly, destructive, and time-consuming (Sattayatewa et al., 2011; American Public Health Association, 2012). For instance, a performance study of this technique reviewing 55 laboratories revealed that around half of the participating laboratories produced inconsistent results, and the coefficient of variation among the reliable laboratories was up to 20% for nitrogen and 60% for phosphorous concentrations (Aminot et al., 1997). Alternatively, Quota models can be fitted to data even when internal quota are not directly monitored (Ducobu et al., 1998; Malerba et al., 2012, 2015). This is possible because the dynamics of internal nutrients in closed systems can sometimes be inferred from population densities and ambient nutrient depletion (Brand, 1991; Fujimoto et al., 1997; De La Rocha et al., 2010). However, this approach is limited to highly controlled laboratory settings and it generally requires more data and more complex experimental designs. Hence, overcoming the limitations involved with direct measurements of cell internal nutrients could substantially enhance our ability to understand and predict dynamics of phytoplankton populations.

The optical properties of a cell can provide important information about the nitrogen utilization of phytoplankton species, as an indirect proxy for their internal nitrogen status. Nitrogen status is known to alter many physiological and morphological aspects of a cell (e.g. cell volume, cell roundness, pigment composition, quantities of internal organelles, concentrations of storage molecules; Vanucci et al., 2010; Adams et al., 2013). Flow cytometric optical analysis provides a means to directly quantify these anatomical and physiological changes that are intrinsically linked to the nitrogen quota of a single cell (Collier, 2000; Dubelaar and Jonker, 2000; Veldhuis and Kraay, 2000). In particular, flow cytometric red fluorescence from four phytoplankton species grown in nitrogen-limited batch cultures explained 77% of the variability in per-cell internal nitrogen, across species and a range of initial nutrient concentrations (Malerba et al., 2016). Monitoring red fluorescence emission from phytoplankton cells has many practical advantages: it is instantaneous, non-destructive, precise, non-biased by inorganic particles, and often routinely measured as part of the protocol for estimating total population densities (Collier, 2000; Dubelaar and Jonker, 2000; Veldhuis and Kraay, 2000). Moreover, it is feasible to separately monitor red fluorescence intensity for mixed species with non-overlapping optical ranges (Trask et al., 1982). Instead, direct methods for total nitrogen quota can only estimate the total elemental composition within a sample. Furthermore, technological advances in nutrient probes and automated submersible flow cytometers (cytobot; Olson et al., 2003) make possible real-time monitoring of phytoplankton dynamics in natural and engineered systems. In contrast, protocols for monitoring total internal nitrogen quota are more complex to automate. However, inferring a state variable from an indirect proxy also requires accounting for an additional source of error, due to the use of a calibration curve to convert between a variable and its proxy. Hence, while incorporating red fluorescence as a proxy for cell nitrogen quota could extend the utilization of Quota models, it is unknown how the added uncertainty of using a calibration curve could affect parameter identifiability, precision, and accuracy when fitting Quota models to phytoplankton time-series.

The aim of the present study was to evaluate the use of flow cytometric red fluorescence in Quota models as a proxy for internal nutrient status. To this end, we conducted two different analyses. In the first analysis, we generated data by simulation, so that the model performance for each fitting approach could be compared using mean squared error (MSE) from the difference between the estimated parameter values and the known, true parameter values used to generate the data. Phytoplankton allometric relationships were used to generate trait values of single species spanning several orders of magnitude in cell size and generate nitrogen-limited time-series for medium nitrogen, internal nitrogen, and total biomass. In the second analysis, Quota models were fitted to real time-series collected from laboratory batch cultures and the accuracy to describe the observed dynamics of internal nitrogen was compared across the three fitting approaches. Both analyses show that incorporating red fluorescence as a proxy for cell nitrogen quota improves the performance of phytoplankton models.

2. Material and methods

2.1. Model development

In this study we derived three approaches to fit Quota models: the Nitrogen-Quota approach, Virtual-Quota approach, and Fluorescence-Quota approach. The three different approaches were derived from the original Quota model by Droop (1973), as:

$$\frac{dN}{dt} = -f\left(N(t)\right)\times B(t) \tag{1a}$$

$$\frac{dQ}{dt} = f\left(N(t)\right) - g\left(Q(t)\right)\times Q(t) \tag{1b}$$

$$\frac{dB}{dt} = g\left(Q(t)\right)\times B(t) \tag{1c}$$

where $N(t)$, $Q(t)$, and $B(t)$ indicate ambient nitrogen, per-cell internal nitrogen quota, and population density, respectively. Functional responses $f\left(N(t)\right)$ and $g\left(Q(t)\right)$ describe the per-cell uptake rate and growth rate as a function of external and internal nitrogen, and are represented with two saturating functional responses:

$$f\left(N(t)\right) = v_{max}\times\frac{N(t)}{N(t)+k} \tag{2a}$$

$$g\left(Q(t)\right) = \mu_{\infty}\times\left(1 - \frac{Q_{min}}{Q(t)}\right) \tag{2b}$$

where v_{max} is per-capita maximum uptake rate, k is the Michaelis–Menten half-saturation constant, μ_{∞} is maximum theoretical growth rate of a cell at infinite nitrogen quota, and Q_{min} is the threshold internal nitrogen concentration at which no cell division occurs.

All three fitting approaches include the state variable $Q(t)$, as the nitrogen quota within a single phytoplankton cell, but differ in the way the model is calibrated to the data. The Nitrogen-Quota approach calibrates the dynamics for $Q(t)$ to direct measurements of per-cell internal nitrogen, as:

$$Q_{obs}(t) = c\times Q(t) \tag{3}$$

where $Q_{obs}(t)$ is the observed nitrogen quota within a single cell, and c is a positive constant accounting for bias associated with laboratory protocols when recording total cell nitrogen in phytoplankton cultures. Directly estimating cell quota has two sources of bias. Firstly, the precision of measuring the elemental composition within a cell depends on the type of chemical bonds within the molecules (e.g. nitrogen atoms connected by double bonds within molecules yield very poor recovery rate with most traditional protocols; Aminot et al., 1997; Raimbault et al., 1999). Secondly, field and laboratory samples often present variable loads of dead cells and nutrient-rich inorganic particles in solution, which contribute to the overall reading and overestimate cell quota in living cells (Shelly et al., 2010). Hence, the parameter c represents underestimated $Q_{obs}(t)$ due to partial N recovery associated with experimental protocol ($c<1$), or overestimated $Q_{obs}(t)$ due to nitrogen recovered from dead cells and suspended inorganic particles within the sample ($c>1$). Bias of up to 50% has been reported with organic nitrogen standards (Nydahl, 1978; Langner and Hendrix, 1982; Raimbault and Slawyk, 1991; Raimbault et al., 1999), so in each simulated dataset c was generated from a uniform distribution ranging between 0.5 and 1.5. The case with no bias in $Q_{obs}(t)$ was also explored, by repeating the analysis with c fixed at 1.

The Fluorescence-Quota approach derives $Q(t)$ from the red fluorescence signal emitted by a cell. Previously, Marra et al. (1990) showed the utility of using red fluorescence as a proxy for internal nutrient status in phytoplankton Quota models. We build on this idea by considering flow cytometric red fluorescence measured from individual cells, instead of total red fluorescence from a volume of water. In this way, the recorded value of red fluorescence signal is determined only by properties of individual cells, without the need to standardize by total population density within the culture (which would introduce additional measurement error). The relationship between $Q(t)$ and per-cell fluorescence intensity was assumed to follow the same power-law functional response documented in Malerba et al. (2016):

$$Q(t) = a\times F(t)^{b} \tag{4}$$

which can be rearranged as:

$$F(t) = \left(\frac{Q(t)}{a}\right)^{\frac{1}{b}} \tag{5}$$

where $F(t)$ indicates the strength of the red fluorescence signal, and a and b are the parameters quantifying the conversion between the two variables.

Finally, the Virtual-Quota approach uses only observations of phytoplankton population size and external nitrate and ammonium concentrations, and infers changes in internal nitrogen $Q(t)$ from the fitted parameter values. This approach to infer $Q(t)$ relies on the assumption that the system is closed. Hence, the sum of the nitrogen in all state variables in Eq. (1a–c) is always constant. In this way, the nitrogen that is depleted from the environment has to be directed to total nitrogen inside the biomass. This leads to a unique set of parameters yielding the best fit between model and data. Such approach is equivalent to Ducobu et al. (1998), Malerba et al. (2012, 2015). Hence, the total number of estimated parameters changes between the three approaches: the Virtual-Quota has 4 trait parameters (v_{∞}, k, μ_{∞}, and Q_{min}), while the Nitrogen-Quota and Fluorescence-Quota have 1 (i.e. c from Eq. (3)) and 2 (i.e. a and b from Eq. (5)) additional parameters, respectively.

Notice that either of the three approaches has strengths and limitations, each with the potential to outperform the others. The Nitrogen-Quota approach is supplied with direct observations for the quota dynamics, but such observations suffer from lack of precision and accuracy. The Virtual-Quota approach estimates parameters only on dynamics for ambient nutrients and population densities, without being influenced by fitting noisy data for internal quota dynamics. However, in this way it is disadvantaged by lower degrees of freedom in the parameter estimates. Finally, the Fluorescence-Quota approach is supplied with data that are indirect and require estimation using a calibration curve, but they represent a more precise and accurate proxy for the real nutrient status of the cell.

2.2. Analysis of simulated data

2.2.1. Data simulation

The Nitrogen-Quota, the Virtual-Quota, and the Fluorescence-Quota approaches were fitted to 100 simulated datasets each. In this way, model performance from each fitting approach could be calculated from the average distance between the parameter values used to generate the data ("true" parameters) and the model estimates calibrated from the same data (estimated parameters). The 100 simulated datasets were generated following these steps:

(1) choose a set of species traits, (2) use stochastic simulations to generate trajectories for external nitrogen, cell nitrogen quota, population density, and red fluorescence, and (3) generate trajectories for 100 days of the corresponding observations of these state variables, incorporating the measurement error for each state variable. Here we describe each step in more detail (please refer to Appendix A for a graphical summary of each step in the analytical methods).

The first step consisted of generating traits representative of phytoplankton species of different sizes. To do that, a cell volume was selected from a uniform distribution on $\log_{10}$-scale from 10^2 to 10^5 μm^3, which is the approximate range reported in Edwards et al. (2012) for freshwater phytoplankton species. Then, the allometric relationships in Edwards et al. (2012) were used to associate the sampled cell volume to expected values for maximum nitrogen uptake (v_{max}), half-saturation rate (k), and minimum nitrogen quota (Q_{min}; see Appendix A and Table S1 in Appendix B). The parameter for maximum theoretical growth rate (μ_∞) of a cell was inferred using the allometric relationships for maximum observed growth rate (μ_{max}) in Edwards et al. (2012) and for maximum nitrogen quota (Q_{max}) in Montagnes and Franklin (2001), and using the formula:

$$\mu_\infty = \mu_{max}\left(1 - \frac{Q_{min}}{Q_{max}}\right) \quad (6)$$

Also, to account for between-species variation around the four allometric relationships, a residual was extracted from the error distribution of each linear regression and added to the expected parameter values (Table S1 in Appendix B).

The second step consisted in simulating the true dynamics of the system using the traits generated in the first step. We did that by using Eq. (1a–c), with the set of trait parameters generated in the first step, to calculate time-series for external nitrogen ($N(t)$), population density ($B(t)$), internal nitrogen ($Q(t)$), and red fluorescence ($F(t)$). Trajectories for the red fluorescence emission (i.e. $F(t)$) of a cell were calculated based on changes in its internal nitrogen status ($Q(t)$) using Eq. (5). The values for a and b were drawn from a bivariate uncertainty distribution from calibration of this relationship using empirical data from four phytoplankton species (Malerba et al., 2016). Log-normally distributed process noise was added to each of the state variables to represent the unexplained variation due to natural stochasticity in the dynamics (Hilborn and Mangel, 1997; Bolker, 2008). The magnitudes of process noise were estimated from calibrating Eq. (1a–c) to empirical data (Malerba et al., 2016). Each time-series was simulated for 100 days, which were sufficient observations to successfully estimate all model parameters with 95% credible intervals. The initial concentration for external nitrogen was standardized as ten times the half-saturation constant (i.e. $10 \times k$) of the species. The initial population density was calculated so that medium nitrogen would become limiting half way through the time-series (i.e. between day 40 and 60). In this way, available nutrients transitioned from N-rich, to N-limited, to N-absent conditions, and growth rates transitioned from fast to zero. Initial populating density was also defined so that population sizes equilibrated by the end of the simulated time-series. Finally, initial per-capita internal nitrogen was randomly selected from a uniform distribution between nitrogen deplete (i.e. $Q(t_o)=Q_{min}$) and nitrogen replete (i.e. $Q(t_o)=Q_{max}$).

The third step consisted of adding observation error to the true system dynamics calculated in step 2. Observation error was added to the dynamics of ambient nitrogen ($N(t)$), observed internal quota ($Q_{obs}(t)$), population density ($B(t)$), and red fluorescence ($F(t)$). The magnitudes of observation error were calculated from the standard deviations of the triplicate independent readings from empirical data in Malerba et al. (2016), which offers an independent estimate for the size of the measurement error for each state variable. The distributions for observed internal quota, population density and red fluorescence were assumed to follow a log-normal distribution, except for medium nitrogen, which was assumed to be normally distributed. The log-normal distribution is appropriate because it constrains all measured values to be positive and because the right-skewed nature of the distribution allows for occasional large positive residuals, which are often observed in population data. Instead, nitrogen was assumed to follow a normal distribution, as observation error make negative concentration values possible when measuring concentrations close to the detection limits of the instrument. Time-series for observed internal quota ($Q_{obs}(t)$) were further modified to account for bias by using Eq. (3) with a value for c sampled from a uniform distribution between 0.5 and 1.5.

The analysis was repeated by modifying the effect of the parameter c, quantifying the magnitude of bias when measuring $Q_{obs}(t)$ from $Q(t)$. Repeating the analysis with no bias in $Q_{obs}(t)$ (i.e. fixing $c=1$) did not change the conclusions of the main analysis (data not shown). This indicates that the Nitrogen-Quota approach to calibrate Quota models is able to accurately estimate c and to account for systematic bias in monitoring $Q(t)$. Notice however that this is only possible when assuming a closed system, where the sum of nitrogen in the three differential equations remain constant. In summary, the bias-effect of the parameter c did not influence the overall performance of the Nitrogen-Quota approach.

After simulating the data for red fluorescence ($F(t)$) and observed internal quota ($Q_{obs}(t)$) and adding process noise and observation error, the recorded relationship between $F(t)$ and $Q_{obs}(t)$ had a mean R^2 of 0.9 across all simulated datasets, which is 15% higher than the corresponding coefficient from empirical data (Malerba et al., 2016). This indicates that a fraction of the observation error in $F(t)$, $Q_{obs}(t)$, or both, was not included in the standard deviations calculated from triplicate independent readings of the samples in Malerba et al. (2016). Therefore, it was necessary to simulate time-series of $F(t)$ and Q_{obs} (t) with an increased observation error estimate (note that process noise does not contribute to the precision of this relationship). It cannot be determined from the data how and where this additional observation error between measurements of $F(t)$ and/or Q_{obs} (t) entered the system. However, details about the experimental protocols provide some indications. Multiple aspects contribute to the overall magnitude of observation error for measuring internal nitrogen quota: the precision when recording reaction intensity (instrumental error), the accuracy of dispensing reagents or diluting samples (manipulative error), and the rate of chemical degradation in all chemical reactions (chemical error). While instrumental and manipulative errors were fully replicated in the experimental methods and thus reflected in the estimate of observation error from the triplicate readings, chemical error can potentially be mis-represented by triplicate readings: the same reagents and stock standards are used at each day, and chemical decay can cause an increase in observation error that is not included in the standard deviations of the replicate measurements. Also, standard stocks for measuring cell internal nitrogen require organic stock standards (e.g. glycine), which are less stable than inorganic controls. Conversely, the observation error associated with measuring red fluorescence only depends on instrumental error, which is well characterized by multiple independent sample readings. In fact, red fluorescence originates from exposing untreated cells to blue light at a wavelength of 488 nm and any inconsistencies involved with handling the sample can only influence cell density estimates, not the red fluorescence emission of a cell. In conclusion, the additional observation error is more likely

to be associated with measuring per-cell internal nitrogen, rather than red fluorescence. However, to be conservative, we added equal proportions of observation error to $F(t)$ and $Q(t)$ until the empirically detected R^2 of 0.77 in Malerba et al. (2016) was reflected in the simulated data.

2.2.2. Model calibration for simulated data

The parameters for maximum nitrogen uptake (v_{max}), half-saturation rate (k), maximum theoretical growth rate (μ_∞), and minimum nitrogen quota (Q_{min}) were estimated with each of the three model fitting approaches for 100 simulated datasets, which were sufficient for analysing trends while keeping computation time in the order of days to weeks (fitting the data from each simulated experiment took between 0.5 and 2 days). Note that the parameter for maximum observed growth rate (μ_{max}) is not part of the Quota model (Eq. (1a–c)) and was therefore not estimated during model calibration. The Nitrogen-Quota approach was calibrated to trajectories of external nitrogen ($N(t)$), population density ($B(t)$), and observed internal quota ($Q_{obs}(t)$), with internal quota ($Q(t)$) estimated from Eq. (3). The Virtual-Quota approach was calibrated only to external nitrogen ($N(t)$) and population density ($B(t)$), with internal quota ($Q(t)$) inferred from changes in $N(t)$ and $B(t)$. The Fluorescence-Quota approach was calibrated to external nitrogen ($N(t)$), population density ($B(t)$), and red fluorescence ($F(t)$), with internal quota ($Q(t)$) estimated from $F(t)$, using Eq. (5). All parameters of the three modelling approaches were estimated assuming uninformative priors, except for the two parameters to regulate the conversion of red fluorescence and internal quota (i.e. a and b) of the Fluorescence-Quota approach, which were calibrated including the priors obtained from the calibration curve in Malerba et al. (2016). This simulates a situation where a preliminary calibration curve was produced between $Red(t)$ and $Q_{obs}(t)$ on a much smaller, independent data set, independently of the $Q_{obs}(t)$ values obtained in the experiments. This approach is convenient, as a calibration curve can be produced using a preliminary experiment involving far fewer measurements of internal nitrogen than would be required to fit models to the full time series data on internal nitrogen directly. Notice however that in this way the Fluorescence-Quota approach is still independent to the Nitrogen-Quota approach, as it is calibrated without using any of the simulated $Q_{obs}(t)$ values.

State-space statistical estimation techniques were used to fit Quota models to each of the 100 datasets per approach. State-space models allow estimating model parameters by simultaneously accounting for both process noise and observation error (Bolker, 2008; Pedersen et al., 2011). The underlying idea behind this modelling technique is that observation error and process noise affect the variability around the model in different ways: the variability caused by observation error will remain constant through time, while the influence of process noise will compound over time. Mathematically this corresponds to:

$$Y_{t+1}^{true} = f\left(Y_t^{true}\right) + \varepsilon \tag{7a}$$

$$Y_{t+1}^{obs} = Y_{t+1}^{true} + \tau \tag{7b}$$

where ε represents the log-normally distributed process noise, τ represents the normally distributed observation error, Y_t^{true} and Y_{t+1}^{true} are the true states of the system at times t and $t+1$, and Y_{t+1}^{obs} is the measured state of the system at time $t+1$ (see Appendix A for more details).

Sampling from the posterior distribution using Bayesian Markov-Chain Monte Carlo (MCMC) is a particularly suitable method to fit state-space models accounting for observation error and process noise. Each dataset was sampled 10^5 times with Gibbs sampler, following 5×10^4 iterations for adapting the chains and 5×10^4 for burn-in, using software JAGS and R with package *rjags* (Plummer, 2003; R Core Team, 2014; Plummer, 2015). To monitor for successful convergence, we visually inspected the iterated history, density plot, and correlation diagram of each chain in each model. Also, we graphically inspect the overlapping posterior distribution between the whole chain and the last 10%, and ensured Geweke z-scores between -2 and 2 (Geweke, 1992). Chains were extended if they failed to meet convergence criteria. Software R was used with packages *coda* and *ggmcmc* for statistical analyses and plots (Plummer et al., 2006; Marín, 2015).

The performance of each model to estimate maximum nitrogen uptake (v_{max}), half-saturation rate (k), maximum theoretical growth rate (μ_∞), and minimum nitrogen quota (Q_{min}) was evaluated using mean squared error (MSE) calculated across all 100 simulations, as:

$$\frac{\sum_{i=1}^{100}\left(\hat{\theta}_i - \theta_i^{true}\right)^2}{100} \tag{8}$$

where θ_i^{true} is the parameter value used to simulate the dataset i, and $\hat{\theta}_i$ is the value of mean of the posterior probability for the parameter estimated from the same dataset. The MSE accounts for both precision and bias to quantify the average distance between the parameter's best-estimate and its true value.

2.2.3. Assumptions of the analytical techniques

This analysis assumes that cell internal nitrogen ($Q(t)$) and cell red fluorescence ($F(t)$) are related in the same way as described in Malerba et al. (2016). The relationship was documented to be linear on a log-log scale, constant across the four species, with a slope of 1.17 (95% CI: 1.05 to 1.29) and an intercept of -18.9 (-19.2 to -18.64), and a goodness-of-fit (R^2) of 0.77. While flow cytometeric red fluorescence in phytoplankton cultures has received relatively little attention compared to other types of red fluorescence (e.g. PAM fluorescence, total fluorescence), a proportionality between red fluorescence within a cell and nutrient status is well-supported in the literature. This is mainly because cells under non-limiting light regimes usually respond to an increase in nitrogen status by producing more pigments (Mulholland and Lomas, 2008; Dortch et al., 1984).

A second assumption involves how the data were simulated. Because the data were simulated with the same model that was used to calibrate the data, the analysis is dependent on the classic Quota model being a good descriptor of the mechanisms regulating the nutrient-limited growth of cells in batch culture conditions. This assumption is robust. The Quota model, first introduced by Droop (1968), is today the most successful type of process-based models to describe nitrogen-limited growth in phytoplankton populations (Pahlow and Oschlies, 2013). However, recent work showed that phytoplankton traits might also not be constants, as assumed by the classic Quota model, but be themselves dependent on internal nutrient status (Verdy et al., 2009; Bonachela et al., 2011). While there is no reason for the conclusions not to apply with these more complex models, further testing should explore the robustness of the present conclusions when including a dependency between quota dynamics and traits.

2.3. Second analysis with laboratory time-series

To test the robustness of the results from simulated data, each of the three fitting approaches were also calibrated to time-series collected by Malerba et al. (2016) from laboratory cultures. Refer to Malerba et al. (2016) for a detailed description of the experimental methods. Briefly, four green algal species (i.e. *Desmodesmus armatus*, *Mesotaenium* sp., *Scenedesmus obliquus*, and *Tetraedron* sp.)

were reared in batch culture conditions under two different initial conditions of medium nitrogen and initial population density. The 8 time-series were 6 or 7 days long and included triplicate daily readings for population density, medium nitrogen, cell internal nitrogen quota, and cell red fluorescence, all collected daily at 18:00 in order to control for any diurnal fluctuations.

The three approaches for fitting Quota models were calibrated to each of the time-series separately, using the same techniques described for the simulated datasets (see section "Model calibration for simulated data"). However, while in the analysis of the simulated datasets we included informative prior distributions for the a and b parameters of the Fluorescence-Quota modelling approach, here we assumed uninformative priors. This is because both the time-series and the calibration curves between $Red(t)$ and $Q_{obs}(t)$ come from the same data reported in Malerba et al. (2016), and this violates the assumption of independence between the dataset and the parameters' prior distributions. Moreover, there were not enough observations in the time-series to simultaneously account for the effects of both process noise and observation error. Therefore, we simplified the analysis by assuming that the residuals in the data were only due to observation error. This assumption is more reasonable than assuming process noise-only, because protocols to monitor per-cell internal nitrogen quota are complex and often suffer from lack of precision (Aminot et al., 1997; Beardall et al., 2001; Shelly et al., 2010).

Differently to simulated data, it is not possible to calculate MSE for model parameters calibrated from laboratory time-series, as the "true" parameter values (θ_{true} in Eq. (5.7)) are unknown. Instead, we assumed that the observations for the internal nitrogen quota represent the "true" dynamics of the internal quota and we tested the ability of each model to fit the observed dynamics. We analysed the coefficient of determination (R^2) between the observed quota and the model-inferred quota for each of the three approaches. Instead of only using the parameter best-estimates, we calculated a distribution of R^2 coefficients by sampling from the posterior distributions of the parameters of each calibrated model. This yields a distribution of R^2 coefficients for each calibrated dataset, which indicates not just the ability of the model to capture the internal nitrogen dynamics, but also how the predictions vary as a result of the combined uncertainties around the parameters.

Note that this way to calculate model performance is biased in favour of the Nitrogen-Quota approach: observations of internal quota ($Q_{obs}(t)$) are used for both calibrating the parameters and for evaluating the performance of the model. This is not the case for the Fluorescence-Quota and Virtual-Quota models, as their calibration is independent to $Q_{obs}(t)$.

3. Results

3.1. Simulated data

The Virtual-Quota approach performed consistently worse than either the Fluorescence-Quota or the Nitrogen-Quota approach for both Mean Squared Error (Fig. 1). All parameters recorded the highest mean squared error when estimated with the Virtual-Quota approach (MSE_{virt}) compared than the Nitrogen-Quota (MSE_{nitr}) and Fluorescence-Quota (MSE_{flu}) approaches (Fig. 1). However, the magnitude of the difference depended on the parameter: the maximum uptake rate (v_{max}) showed the least difference between approaches ($< 10\%$), while the half-saturation constant (k), minimum quota (Q_{min}), and the maximum theoretical growth rate (μ_∞) where up to 1 and 2 orders of magnitude higher for the MSE_{virt} compared to MSE_{nitr} and MSE_{flu}, respectively (Fig. 1). Hence, inferring internal nitrogen dynamics from external nitrogen depletion and population density (i.e. Virtual-Quota approach) led to less accuracy and less precision compared to including measurements of internal nitrogen or of red fluorescence.

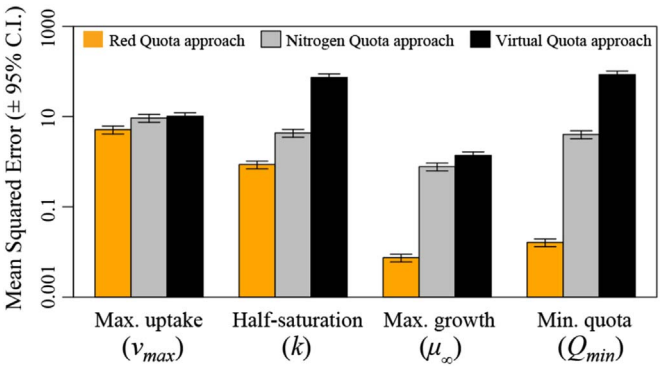

Fig. 1. Mean Squared Error for per-capita maximum uptake rate (v_{max}), Michaelis–Menten half-saturation constant (k), maximum theoretical growth rate (μ_∞), and minimum cell nitrogen quota (Q_{min}), calibrated with the three alternative approaches to fit Quota models. Mean Squared Error was calculated from 100 calibrated datasets for each model as $mean\left[\left(\hat{\theta} - \theta_{true}\right)^2\right]$, where θ_{true} is the value used to generate the data and $\hat{\theta}$ is the mean parameter value estimated from the data.

3.2. Laboratory time-series

All three approaches fit the eight laboratory time-series for medium nitrogen and population density very accurately and with comparable precision (most R^2 higher than 0.8; see panels A, B, D, E in Fig. S1-4 in Appendix C). The exception was the second dataset for *Tetraedron* sp., where all three models predicted dynamics for population density that showed substantial lack of fit (Fig. S4 E). This lack of fit is due to a decrease in the rate of population growth from day 1 that did not correspond to an increase in degree of nitrogen limitation in the system (most ambient nitrogen was still available). This violates the assumption of Quota models that nitrogen is the only limiting factor for cell growth.

Conversely, the performance of the Quota model to predict internal nitrogen dynamics differs considerably across fitting approaches (Fig. 2). The mean goodness-of-fit across the 8 datasets between model-inferred quota dynamics and observations on internal nitrogen was highest in the Nitrogen-Quota approach ($R^2 = 0.55$), followed by the Fluorescence-Quota approach ($R^2 = 0.47$) and the Virtual-Quota approach ($R^2 = 0.32$; Fig. 2 B). It is important to notice that all R^2 coefficients for the Virtual-Quota approach were affected by wider credible intervals compared to either the Nitrogen-Quota or the Fluorescence-Quota approaches (Fig. 2). This indicates that the Nitrogen-Quota or the Fluorescence-Quota approaches could predict the dynamics of internal nitrogen more accurately and with less uncertainty, compared to the Virtual-Quota approach.

Overall, the results from fitting real time-series are mostly in agreement with the analysis of simulated dynamics. The lower mean squared error for Nitrogen-Quota and the Fluorescence-Quota approaches with simulated data (Fig. 1) is consistent with both their higher mean and lower uncertainty of R^2 with real time-series (Fig. 2), compared to the Virtual-Quota approach.

4. Discussion

This study showed that including per-cell red fluorescence as a proxy for internal N (Fluorescence-Quota approach) can improve the performance of Quota models while still accounting for the ability of cells to store nitrogen intracellularly. Furthermore,

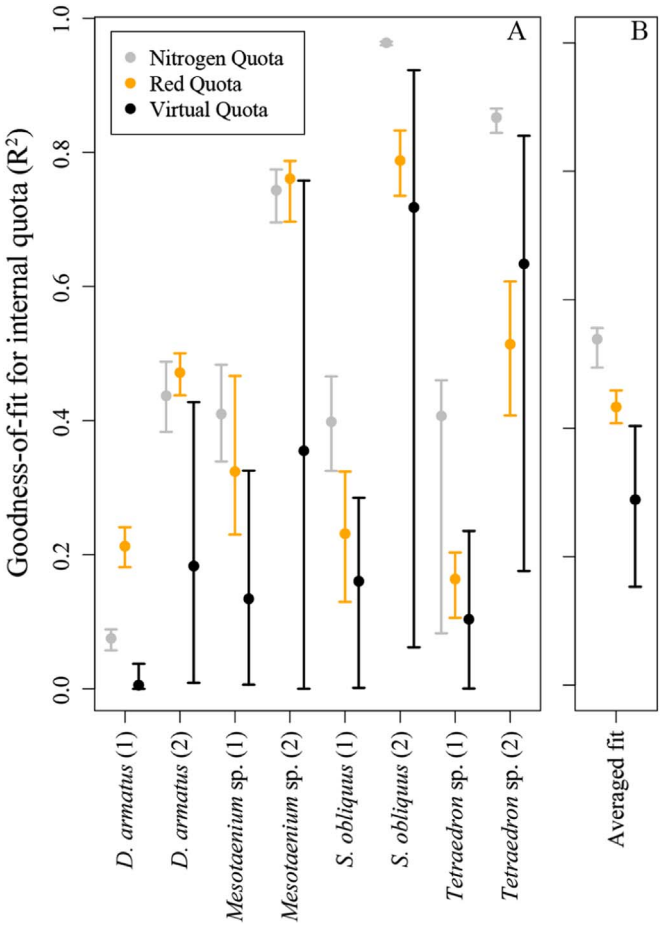

Fig. 2. Goodness-of-fit coefficients (R^2) between observed and predicted dynamics of internal nitrogen for (A) two initial conditions for each of the 4 green algal species (*Desmodesmus armatus*, *Mesotaenium* sp., *Scenedesmus obliquus*, and *Tetraedron* sp.) reared in laboratory batch cultures and (B) the weighted mean across all eight R^2 scores. The 95% credible intervals for R^2 were calculated by integrating over the posterior distribution of the calibrated parameters of each of the model. The R^2 scores were calculated from the model fits represented in panels C and F of Fig. S1–S4 in Appendix C.

simulated data showed that the higher instrumental precision for red fluorescence, compared to measuring internal nitrogen directly, makes the Fluorescence-Quota approach superior even to the classic Nitrogen-Quota approach.

The many advantages of measuring red auto-fluorescence from single cells make the proposed Fluorescence-Quota approach a promising way to reduce some of the limitations of modelling phytoplankton dynamics. This study is only the first attempt to integrate an indirect proxy for the study of nutrient utilization in phytoplankton and much uncertainty still remains on the robustness of this technique. For instance, a relationship between red fluorescence and the quota of the most limiting nutrient of a cell has been only documented for nitrogen-limited laboratory cultures (Malerba et al., 2016). However, a decrease in pigmentation should in principle arise also in cells limited by other macronutrients. This is due to a relocation of elements in short demand from pigments and storage molecules to vital metabolic functions (Mulholland and Lomas, 2008; Dortch et al., 1984). Consistently, studies on taxonomically unrelated phytoplankton species reared in laboratory batch cultures show positive trends in flow cytometric optical values when cells are replete with iron, phosphorous, and silicon (Cleveland and Perry, 1987; Demers et al., 1989; Zettler et al., 1996; Timmermans et al., 2001; Davey et al., 2008; Liu and Qiu, 2012). Hence, there is potential to extend this approach also to different limiting nutrients, starting by testing for proportionality between optical properties and internal status of a cell reared when limited by different nutrients.

Laboratory studies have documented factors other than nitrogen status that can affect the phenomenon of phytoplankton chlorophyll fluorescence, such as light intensity, diel cycle, pigment composition, and other limiting nutrients (Sosik et al., 1989; DuRand and Olson, 1998; Mas et al., 2008). However, the analysis of per-cell fluorescence has received relatively little attention compared to other types of fluorescence (e.g. total fluorescence, Pulse Amplitude Modulated fluorometry), as the use of flow cytometers was established in phytoplankton ecology relatively recently (Veldhuis and Kraay, 2000; Sosik et al., 2010). Flow cytometers automatically record fluorescence intensity whenever they are used to estimate the population density of a phytoplankton sample. At present, time-series of per-cell red fluorescence are rarely of interest and scientific publications mostly do not report them. New evidence indicates that flow cytometric red fluorescence can not only reveal physiological mechanisms of a cell but also improve current phytoplankton models (Malerba et al., 2016). Promoting the publication and use of per-cell red fluorescence data can provide more opportunities for further verification and a better evaluation of using flow cytometric fluorescence proxies in phytoplankton models.

Another potential application emerging from this research is the use of red fluorescence for studying cell internal nitrogen from individual species when reared in mixed cultures. Direct estimation using traditional laboratory protocols cannot allow separately monitoring nutrient storages of mixed species. Conversely, indirect estimation from optical properties of mixed phytoplankton species with non-overlapping values can easily be partitioned, quantifying the contribution of each individual species (Trask et al., 1982; Petersen et al., 2012). There is a large body of theoretical work examining the role of resource storage in community ecology and its interaction with temporal and spatial variability (Grover, 2011; Grover et al., 2012). This methodology to calibrate Quota models from laboratory time-series may help to test theoretical predictions with empirical laboratory experiments.

Our study presents a novel approach to incorporating and evaluating indirect proxies in dynamic models. Specifically, present findings showed that red fluorescence could substantially improve the estimation of phytoplankton traits when fitting process-based Quota models to time-series data. Many other population models incorporate variables representing the condition of individual organisms. For instance, Dynamic Energy Budget models rely on the assumption that energy and resources can be stored within organisms (Nisbet et al., 2000; Kooijman, 2010). However, variables characterizing the internal condition of individuals often require destructive and time-consuming laboratory protocols, or they may simply be impossible to measure directly (e.g. separate energy reserves for growth, reproduction, or maintenance of an individual). Consequently, most dynamic models infer changes in internal storages without testing these implied dynamics against data (i.e., they are unobserved state variables). This practice impairs the capacity to validate model performance, and it increases parameter uncertainty. Therefore, the approach applied here to evaluate an internal nitrogen proxy in phytoplankton may also be useful more broadly, for evaluating indirect proxies in other populations for which difficult-to-measure internal states strongly influence population dynamics.

Acknowledgements

This research was supported by AIMS@JCU (aims.jcu.edu.au), the Australian Institute of Marine Science (www.aims.gov.au), and

James Cook University (www.jcu.edu.au).

We are grateful to the Ecological Modelling Research Group at James Cook University, especially Dr. Loic Thibaut for comments on modelling techniques and R codes. We also thank the High Performance Computing team at James Cook University.

Appendix A. Supplementary material

Supplementary data associated with this article can be found in the online version at http://dx.doi.org/10.1016/j.jtbi.2016.05.023.

References

Adams, C., Godfrey, V., Wahlen, B., Seefeldt, L., Bugbee, B., 2013. Understanding precision nitrogen stress to optimize the growth and lipid content tradeoff in oleaginous green microalgae. Bioresour. Technol. 131, 188–194.

American Public Health Association, 2012. Standard Methods for the Examination of Water and Wastewater, 22nd edition. APHA-AWWA-WEF, Washington, DC.

Aminot, A., Kirkwood, D., Carlberg, S., 1997. The QUASIMEME laboratory performance studies (1993–1995): overview of the nutrients section. Mar. Pollut. Bull. 35, 28–41.

Beardall, J., Young, E., Roberts, S., 2001. Approaches for determining phytoplankton nutrient limitation. Aquat. Sci. 63, 44–69.

Bolker, B., 2008. Dynamic Models. Ecological Models and Data in R. In: Bolker, B. (Ed.), 2008. Princeton University Press, Princeton, NJ..

Bonachela, J.A., Raghib, M., Levin, S.A., 2011. Dynamic model of flexible phytoplankton nutrient uptake. Proc. Natl. Acad. Sci. USA 108, 20633–20638.

Brand, L.E., 1991. Minimum iron requirements of marine phytoplankton and the implications for the biogeochemical control of new production. Limnol. Oceanogr. 36, 1756–1771.

Brown, J.H., Gillooly, J.F., Allen, A.P., Savage, V.M., West, G.B., 2004. Toward a metabolic theory of ecology. Ecology 85, 1771–1789.

Caperon, J., Meyer, J., 1972. Nitrogen-limited growth of marine phytoplankton—II. Uptake kinetics and their role in nutrient limited growth of phytoplankton. Deep Sea Res. Oceanogr. Abstr. 19, 619–632.

Caro, T., 2010. Conservation by Proxy: Indicator, Umbrella, Keystone, Flagship, and Other Surrogate Species. Island Press, Washington, DC.

Cleveland, J.S., Perry, M.J., 1987. Quantum yield, relative specific absorption and fluorescence in nitrogen-limited chaetoceros-gracilis. Mar. Biol. 94, 489–497.

Collier, J.L., 2000. Flow cytometry and the single cell in phycology. J. Phycol. 36, 628–644.

Davey, M., Tarran, G.A., Mills, M.M., Ridame, C., Geider, R.J., LaRoche, J., 2008. Nutrient limitation of picophytoplankton photosynthesis and growth in the tropical north atlantic. Limnol. Oceanogr. 53, 1722–1733.

De La Rocha, C.L., Terbruggen, A., Volker, C., Hohn, S., 2010. Response to and recovery from nitrogen and silicon starvation in *Thalassiosira weissflogii*: growth rates, nutrient uptake and C, Si and N content per cell. Mar. Ecol. Prog. Ser. 412, 57–68.

Demers, S., Davis, K., Cucci, T.L., 1989. A flow cytometric approach to assessing the environmental and physiological status of phytoplankton. Cytometry 10, 644–652.

Dempster, T., Sanchez-Jerez, P., Fernandez-Jover, D., Bayle-Sempere, J., Nilsen, R., Bjorn, P.A., Uglem, I., 2011. Proxy measures of fitness suggest coastal fish farms can act as population sources and not ecological traps for wild gadoid fish. Plos One 6, e15646.

Dortch, Q., Clayton, J.R., Thoresen, S.S., Ahmed, S.I., 1984. Species-differences in accumulation of nitrogen pools in phytoplankton. Mar. Biol. 81, 237–250.

Droop, M.R., 1973. Some thoughts on nutrient limitation in algae. J. Phycol. 9, 264–272.

Droop, M.R., 1983. 25 years of algal growth-kinetics – a personal view. Botanica Mar. 26, 99–112.

Dubelaar, G.B.J., Jonker, R.R., 2000. Flow cytometry as a tool for the study of phytoplankton. Sci. Mar. 64, 135–156.

Ducobu, H., Huisman, J., Jonker, R.R., Mur, L.R., 1998. Competition between a prochlorophyte and a cyanobacterium under various phosphorus regimes: comparison with the Droop model. J. Phycol. 34, 467–476.

DuRand, M.D., Olson, R.J., 1998. Diel patterns in optical properties of the chlorophyte *Nannochloris* sp.: relating individual-cell to bulk measurements. Limnol. Oceanogr. 43, 1107–1118.

Edwards, K.F., Thomas, M.K., Klausmeier, C.A., Litchman, E., 2012. Allometric scaling and taxonomic variation in nutrient utilization traits and maximum growth rate of phytoplankton. Limnol. Oceanogr. 57, 554–566.

Eigenbrod, F., Armsworth, P.R., Anderson, B.J., Heinemeyer, A., Gillings, S., Roy, D.B., Thomas, C.D., Gaston, K.J., 2010. The impact of proxy-based methods on mapping the distribution of ecosystem services. J. Appl. Ecol. 47, 377–385.

Epstein, H.E., Raynolds, M.K., Walker, D.A., Bhatt, U.S., Tucker, C.J., Pinzon, J.E., 2012. Dynamics of aboveground phytomass of the circumpolar Arctic tundra during the past three decades. Environ. Res. Lett., **7**.

Fujimoto, N., Sudo, R., Sugiura, N., Inamori, Y., 1997. Nutrient-limited growth of *Microcystis aeruginosa* and *Phormidium tenue* and competition under various N: P supply ratios and temperatures. Limnol. Oceanogr. 42, 250–256.

Geweke, J.F., 1992. Evaluating the accuracy of sampling-based approaches to the calculation of posterior moments. In: Berger, J.O., Bernardo, J.M., Dawid, A.P., Smith, A.F.M. (Eds.), Bayesian Statistics vol. 4. Clarendon Press, Oxford, UK.

Grover, J.P., 2011. Resource storage and competition with spatial and temporal variation in resource availability. Am. Nat. 178, E124–E148.

Grover, J.P., Hsu, S.B., Wang, F.B., 2012. Competition between microorganisms for a single limiting resource with cell quota structure and spatial variation. J. Math. Biol. 64, 713–743.

Hilborn, R., Mangel, M., 1997. The Ecological Detective: Confronting Models with Data. Princeton University Press, Chichester, Princeton, NJ.

Holmborn, T., Dahlgren, K., Holeton, C., Hogfors, H., Gorokhova, E., 2009. Biochemical proxies for growth and metabolism in *Acartia bifilosa* (Copepoda, Calanoida). Limnol. Oceanography: Methods 7, 785–794.

Kooijman, S.A.L.M., 2010. Dynamic Energy Budget Theory for Metabolic Organisation, 3rd ed Cambridge University Press.

Langner, C.L., Hendrix, P.F., 1982. evaluation of a persulfate digestion method for particulate nitrogen and phosphorus. Water Res. 16, 1451–1454.

Leadbeater, B.S., 2006. The 'Droop Equation' – Michael Droop and the legacy of the 'Cell-Quota Model' of phytoplankton growth. Protist 157, 345–358.

Li, Q., Zhang, H., Du, X., Wen, N., Tao, Q., 2014. County-level rice area estimation in southern China using remote sensing data. J. Appl. Remote Sens., 8.

Lindenmayer, D., Barton, P., Pierson, J., 2015. Indicators and Surrogates of Biodiversity and Environmental Change. CSIRO Publishing.

Liu, S.W., Qiu, B.S., 2012. Different responses of photosynthesis and flow cytometric signals to iron limitation and nitrogen source in coastal and oceanic synechococcus strains (cyanophyceae). Mar. Biol. 159, 519–532.

Madin, J.S., Baird, A.H., Dornelas, M., Connolly, S.R., 2014. Mechanical vulnerability explains size-dependent mortality of reef corals. Ecol. Lett. 17, 1008–1015.

Malerba, M.E., Connolly, S.R., Heimann, K., 2012. Nitrate-nitrite dynamics and phytoplankton growth: formulation and experimental evaluation of a dynamic model. Limnol. Oceanogr. 57, 1555–1571.

Malerba, M.E., Connolly, S.R., Heimann, K., 2015. An experimentally validated nitrate-ammonium-phytoplankton model including effects of starvation length and ammonium inhibition on nitrate uptake. Ecol. Modell. 317, 30–40.

Malerba, M.E., Connolly, S.R., Heimann, K., 2016. Standard flow cytometry as a rapid and non-destructive proxy for cell nitrogen quota. J. Appl. Phycol. 28, 1085–1095.

Marín, X.F.I., 2015. ggmcmc: Graphical tools for analyzing Markov Chain Monte Carlo simulations from Bayesian inference, ⟨http://xavier-fim.net/packages/ggmcmc⟩.

Marra, J., Bidigare, R.R., Dickey, T.D., 1990. Nutrients and mixing, chlorophyll and phytoplankton growth. Deep-Sea Res. Part A: Oceanogr. Res. Pap. 37, 127–143.

Mas, S., Roy, S., Blouin, F., Mostajir, B., Therriault, J.C., Nozais, C., Demers, S., 2008. Diel variations in optical properties of *Imantonia rotunda* (haptophyceae) and *Thalassiosira pseudonana* (Bacillariophyceae) exposed to different irradiance levels. J. Phycol. 44, 551–563.

McGill, B.J., Enquist, B.J., Weiher, E., Westoby, M., 2006. Rebuilding community ecology from functional traits. Trends in Ecol. and Evol. 21, 178–185.

Montagnes, D.J.S., Franklin, D.J., 2001. Effect of temperature on diatom volume, growth rate, and carbon and nitrogen content: reconsidering some paradigms. Limnol. Oceanogr. 46, 2008–2018.

Mulholland, M.R., Lomas, M.W., 2008. Nitrogen uptake and assimilation. In: Capone, D.G., Bronk, D.A., Mulholland, M.R., Carpenter, E.J. (Eds.), Nitrogen in Marine Environment. Elsevier, pp. 303–384.

Nisbet, R.M., Muller, E.B., Lika, K., Kooijman, S.A.L.M., 2000. From molecules to ecosystems through dynamic energy budget models. J. Anim. Ecol. 69, 913–926.

Nydahl, F., 1978. On the peroxodisulphate oxidation of total nitrogen in waters to nitrate. Water Res. 12, 1123–1130.

Olson, R.J., Shalapyonok, A., Sosik, H.M., 2003. An automated submersible flow cytometer for analyzing pico- and nanophytoplankton: FlowCytobot. Deep-Sea Res. Part I – Oceanogr. Res. Pap. 50, 301–315.

Pahlow, M., Oschlies, A., 2013. Optimal allocation backs Droop's cell-quota model. Mar. Ecol. Prog. Ser. 473, 1–5.

Pedersen, M.W., Berg, C.W., Thygesen, U.H., Nielsen, A., Madsen, H., 2011. Estimation methods for nonlinear state-space models in ecology. Ecol. Modell. 222, 1394–1400.

Pereira Coltri, P., Zullo, J., Ribeiro do Valle Goncalves, R., Romani, L.A.S., Pinto, H.S., 2013. Coffee crop's biomass and carbon stock estimation with usage of high resolution satellites images. IEEE J. Select. Topics Appl. Earth Observ. Remote Sens. 6, 1786–1795.

Petersen, T.W., Brent Harrison, C., Horner, D.N., van den Engh, G., 2012. Flow cytometric characterization of marine microbes. Methods 57, 350–358.

Plummer, M., 2003. JAGS: A Program for Analysis of Bayesian Graphical Models using Gibbs sampling.

Plummer, M., 2015. rjags: Bayesian Graphical Models using MCMC. R package version 3-15. ⟨http://CRAN.R-project.org/package=rjags⟩.

Plummer, M., Best, N., Cowles, K., Vines, K., 2006. CODA: convergence diagnosis and output analysis for MCMC. R. News 6, 7–11.

R Core Team, 2014. R: A Language and Environment for Statistical Computing. R Foundation for Statistical Computing, Vienna, Austria. (URL) ⟨http://www.R-project.org/⟩.

Raimbault, P., Pouvesle, W., Diaz, F., Garcia, N., Sempere, R., 1999. Wet-oxidation and automated colorimetry for simultaneous determination of organic carbon, nitrogen and phosphorus dissolved in seawater. Mar. Chem. 66, 161–169.

Raimbault, P., Slawyk, G., 1991. A semiautomatic, wet-oxidation method for the determination of particulate organic nitrogen collected on filters. Limnol. Oceanogr. 36, 405–408.
Runge, J.A., Roff, J.C., 2000. The measurement of growth and reproductive rates. In: Harris, R., Wiebe, P., Lenz, J., Skjoldal, H.R., Huntley, M. (Eds.), ICES Zooplankton Methodology Manual. Academic Press, San Diego, pp. 401–454.
Salin, K., Auer, S.K., Rey, B., Selman, C., Metcalfe, N.B., 2015. Variation in the link between oxygen consumption and ATP production, and its relevance for animal performance. Proc. R. Soc. B: Biol. Sci. 282.
Santin-Janin, H., Garel, M., Chapuis, J.L., Pontier, D., 2009. Assessing the performance of NDVI as a proxy for plant biomass using non-linear models: a case study on the Kerguelen archipelago. Polar Biol. 32, 861–871.
Sattayatewa, C., Arnaldos, M., Pagilla, K., 2011. Measurement of organic nitrogen and phosphorus fractions at very low concentrations in wastewater effluents. Water Environ. Res. 83, 675–683.
Shelly, K., Holland, D., Beardall, J., 2010. Assessing nutrient status of microalgae using chlorophyll a fluorescence. In: Suggett, D.J., Borowitzka, M., Prášil, O. (Eds.), Chlorophyll a Fluorescence in Aquatic Sciences Methods and Applications. Springer, New York, pp. 223–236.
Son, N.T., Chen, C.F., Chen, C.R., Minh, V.Q., Trung, N.H., 2014. A comparative analysis of multitemporal MODIS EVI and NDVI data for large-scale rice yield estimation. Agric. For. Meteorol. 197, 52–64.
Sosik, H.M., Chisholm, S.W., Olson, R.J., 1989. Chlorophyll fluorescence from single cells – interpretation of flow cytometric signals. Limnol. Oceanogr. 34, 1749–1761.
Sosik, H.M., Olson, R.J., Armbrust, E.V., 2010. Flow cytometry in phytoplankton research. In: Suggett, D.J., Borowitzka, M., Prášil, O. (Eds.), Chlorophyll a Fluorescence in Aquatic Sciences Methods and Applications. Springer, New York, pp. 223–236.
Stephens, P.A., Pettorelli, N., Barlow, J., Whittingham, M.J., Cadotte, M.W., 2015. Management by proxy? The use of indices in applied ecology. J. Appl. Ecol. 52, 1–6.
Trask, B.J., Engh, G.Jvd, Elgershuizen, J.H.B.W., 1982. Analysis of phytoplankton by flow cytometry. Cytometry 2, 258–264.
Timmermans, K.R., Davey, M.S., Wagt, B., v.d., Snoek, J., Geider, R.J., Veldhuis, M.J.W., Gerringa, L.J.A., Baar, H.J.Wd, 2001. Co-limitation by iron and light of *chaetoceros brevis*, *C. dichaeta* and *C. calcitrans* (bacillariophyceae). Mar. Ecol. Prog. Ser. 217, 287–297.
Vanucci, S., Guerrini, F., Milandri, A., Pistocchi, R., 2010. Effects of different levels of N- and P-deficiency on cell yield, okadaic acid, DTX-1, protein and carbohydrate dynamics in the benthic dinoflagellate Prorocentrum lima. Harmful Algae 9, 590–599.
Veldhuis, M.J.W., Kraay, G.W., 2000. Application of flow cytometry in marine phytoplankton research: current applications and future perspectives. Sci. Mar. 64, 121–134.
Verdy, A., Follows, M., Flierl, G., 2009. Optimal phytoplankton cell size in an allometric model. Mar. Ecol. Prog. Ser. 379, 1–12.
Violle, C., Navas, M.-L., Vile, D., Kazakou, E., Fortunel, C., Hummel, I., Garnier, E., 2007. Let the concept of trait be functional!. Oikos 116, 882–892.
Zettler, E.R., Olson, R.J., Binder, B.J., Chisholm, S.W., Fitzwater, S.E., Gordon, R.M., 1996. Iron-enrichment bottle experiments in the equatorial pacific: responses of individual phytoplankton cells. Deep-Sea Res. Part II – Topical Stud. Oceanogr. 43, 1017–1029.